Indian Journal of Pure & Applied Physics
Vol. 44, September 2006, pp. 661-669

Development of an experimental arrangement for precise measurement of angular distribution of ultrasound scattering

Ratan K Saha†, Manas K Roy* ,Subhajit Karmakar, Saibal Saha & Swapan K Sen

Saha Institute of Nuclear Physics, 1/AF Bidhannagar, Kolkata 700 064

*Sateyendra Nath Bose National Centre of Basic Sciences, Block JD, Sector III, Salt Lake, Kolkata 700 064

*E-mail:ratank.saha@saha.ac.in

Received 8 March 2006; revised 4 July 2006; accepted 14 July 2006

This paper describes step-by-step development of a custom-made measurement system and also provides an assessment of the reliability of the set-up. The angular distribution of the scattered field generated by a sufficiently long cylindrical scatterer in water medium has been measured by this system. The measured values have been compared with the theoretical results to validate the instrument. The theoretical curves have been obtained by using the Faran's theory [*J Acoust Society of America*, 23(4) (1951) 405]. In this study, an acoustic wave of frequency 2.19 MHz emitted by a medical ultrasound source has been employed to provide energy to the scattering object. Two steel wires of different gauges (0.68mm and 0.91mm in diameter) with size parameters k$a \approx 3.12$ and 4.17, respectively, have been taken as prototype scatterers. Here, k is the wave number of the incident wave and a is the radius of the target. Our results show that the system is stable, capable of precise scattering measurements and measured values are reproducible. The system has also the flexibility of incorporating scatters of different shapes and also ultrasound probes of different frequencies.

Keywords: Ultrasound scattering, Pulse-echo imaging, Ultrasound
IPC Code: A61N7/00

1 Introduction

Ultrasound scattering is an established technique in a number of domains[1]. It has wide range of applications in industry for flaw detection and quality control, in oceanography for underwater studies, in mining for particle size distribution in colloids and emulsions[2-4]. The back scattering or pulse-echo technique has been employed to characterize biological tissue medium and to image soft tissue structures for the purpose of medical diagnosis[5,6] . This technique is being used as an important diagnostic tool and has no deleterious effects[7] . However, the pulse-echo imaging highly depends on operator's efficiency and scanning procedures. Hence, a new imaging technique, which is known as quantitative imaging, has gained more importance among diagnostic researchers because it can provide an image free from unwanted effects[6,8]. One of the methods[6] of quantitative imaging, namely, scatter imaging utilizes the scattered signal to produce quantitative maps of tissue interaction parameters.

Inspired by the extensive area of applications of ultrasound scattering techniques the present authors have undertaken the development of a system for the measurement of angular scattered components of ultrasound. During its development, care has been taken to specify various design parameters, namely, angular resolution, dimensions of various functional parts etc. Of course, these parameters have been selected on the basis of interrogating frequency range and nature of our future work, for instance, scattering by an isolated particle or by a number of scatterers belonging to a bulk sample. In this paper, a thorough description of the underlying instrumentations of the back and angular scatter ultrasound field measuring system has been presented. The reproducibility of measured data, angular accuracy and stability of the system have been extensively studied experimentally and corresponding results are also reported in this paper. The underlying theory for scattering by a long cylindrical object and the corresponding experiment carried out to examine the suitability and compatibility of the set-up for angular scattering measurements.

2 Scattering by a Long Rigid Cylinder

The exact analytical solution for the scattering of a plane wave by a long homogeneous cylinder can be obtained by using partial wave analysis. The solution through this method can be derived by expanding the incident plane wave in terms of Bessel's functions of various orders (in view of the cylindrical symmetry of

the scatterer) and using the fact that the normal component of particle velocity and acoustic pressure must be continuous at the scatterer surface. To calculate the normal component of particle velocity and acoustic pressure within the scatterer one has to consider contributions from longitudinal and shear waves for a rigid scatterer, as both waves can propagate through it. Faran[1] in 1951 first obtained the exact solution for the scattered field by including the effects of shear waves. In this context, it is worth mentioning that these types of scattering objects were previously treated as immovable and impenetrable scatterers and as a consequence, the corresponding theoretical scattering patterns[9] were unable to reproduce the experimental results. However, the angular scattering patterns based on the Faran's theory are in excellent agreement with the experimental results.

The top view of a typical scattering geometry is depicted in Fig. 1 where the centre of circular cross-section of the cylinder is taken as the origin of the coordinate system and this particular choice simplifies the mathematical formulation. The scattered wave in the asymptotic region for an incident plane-interrogating wave with wave vector (**k**) perpendicular to the axis of a cylindrically symmetric scatterer may be expanded in terms of the trigonometric function[1] .

$$p_s(\mathbf{r}) = P_0\sqrt{\frac{2}{\pi k}}\sum_{m=0}^{\infty}\varepsilon_m \sin\eta_m \exp(i\eta_m) \times \cos(m\varphi)\frac{\exp(i\mathbf{k}.\mathbf{r})}{\sqrt{r}} \quad \ldots (1)$$

The subscript *s* indicates the scattered wave. It is evident from Eq. (1) that, when it is viewed at a distance far away from the centre of the cylinder, the scattered wave is essentially a cylindrical wave (or a two-dimensional wave) with its intensity falling off 1/*r*. Here, P_0 is the amplitude of the incident wave and ε_m is the Neumann constant with, ε_m=1 if *m=0,* else ε_m=2. The direction of the detector makes an azimuthal angle φ with **k** and also the detector is placed at a distance *r* from the origin of the coordinate system. The phase shift of the m^{th} partial wave is given by η_m, which is a function of the density, longitudinal speed of sound and Poisson's ratio of the scattering object, density and longitudinal speed of sound in the surrounding medium. Furthermore, it is also a function of the size parameter, $x = ka$, where k is the magnitude of **k** and a is the radius of the cylindrical target. Modulus of the amplitude of the scattered wave in the direction φ with respect to the incident wave and at a distance **r** from the centre divided by the incident amplitude P_0 is given by,

$$\left|p_s(\mathbf{r})\right| = \sqrt{\frac{2}{\pi kr}}\left|\sum_{m=0}^{\infty}\varepsilon_m \sin\eta_m \exp(i\eta_m)\cos(m\varphi)\right|, \quad \ldots(2)$$

which is the quantity of interest from the point of view of measurement.

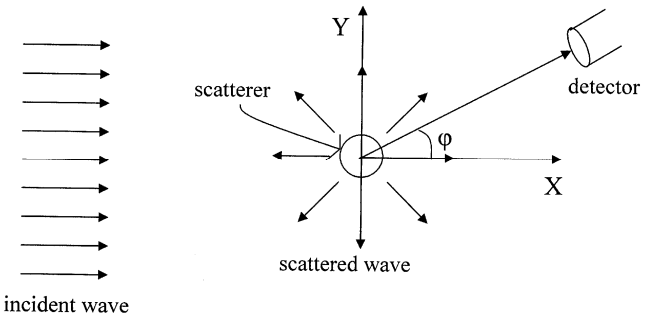

Fig. 1—Scattering of plane wave by a homogenous and infinitely long cylinder (top view).

3 Development of the System

An elaborate description showing dimensions of various functional parts of the system designed and fabricated for the scattering measurement is presented in Fig. 2. The set-up consists of two major components: (i) The tank which contains the water medium and ii) the angular positioning system for accurate placement of the receiver.

The development of such a system begins with the specifications of dimensions of the tank and those in turn also set the dimensions of the angular positioning system. The minimum length of a tank mainly depends upon the input frequency range, which will be used for the purpose of future investigations. For example, if the interrogative frequency range is 2-10 MHz, then the corresponding length of the near field zone (NFZ) in water medium can be calculated to be 30.72 to 153.60 mm for a transducer having diameter 9.6 mm where the velocity of ultrasound in water medium is taken as 1500m/s. This length may even increase for transducers with higher aperture sizes. Further, a typical PANAMETRICS-NDT, V325 transducer along with its specially designed Bayonet Neill-Concelman (BNC) connector is ≈ 73.5 mm long. This connector is suitable for underwater electrical connections. Hence, half length of the tank

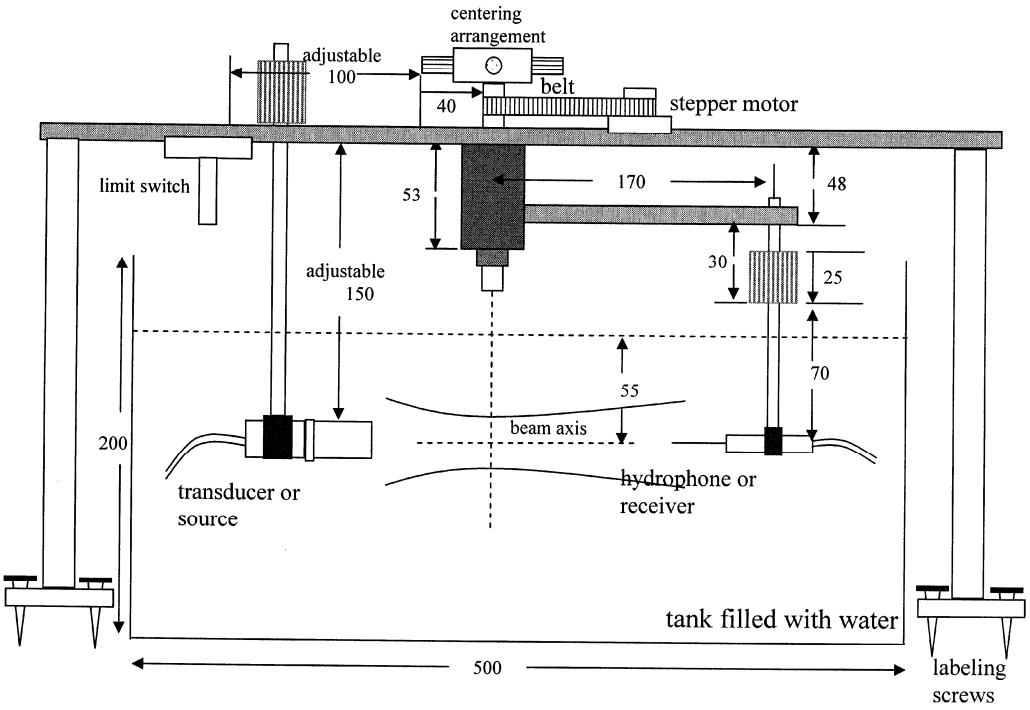

Fig. 2—Detail dimensional description of the set-up from side view (length unit is mm and lengths are not scaled).

becomes around 130 to 250 mm for this frequency range if the source transducer is placed in such a way that only far field scattering is allowed and if some space is left for the electrical cable (of about 30 mm) behind the source as shown in Fig. 2. In general, the scatterer is placed near the central portion of the tank and that has also been adhered to here. Accordingly, we have fixed 500 mm as the length of the tank. Correspondingly, the breadth is also taken as 500 mm for our case so that we can place the hydrophone at a distance sufficiently far from the scatterer to receive the scattered field in the asymptotic region, as required for Eq. (2) to be valid. Due to the finite size of the tank, reflection of the incident pulse occurs. Nevertheless, the incident pulse or scattered pulse can be separated from the reflected pulse by employing proper time domain gating. The height of the tank has been taken as 200 mm and hence, the scattering plane remains at a reasonable depth from the water surface during the experiment. This depth is generally estimated by the beam diameter, otherwise, direct beam may interfere with the reflected beam, from the water surface, at the point of reception. For instance, half-width of the main lobe can be calculated to be ≈ 2.94 mm at focal planes for this frequency range and corresponding angle of divergence varies from 5.46° to 1.09°. The half-width also increases as the distance from the transducer increases.

One of the major parts of the angular positioning system is the transducer holder. We have made a horizontally guided transducer holder whose diameter is slightly greater than that of BNC. BNC is common for all transducers and therefore a single transducer holder is sufficient for operations in the whole frequency range. Furthermore, BNC can be gripped properly with the holder along the guide by tightening the side screw arrangement. In our system, the holder can move in directions both parallel and perpendicular to that of the incident beam to facilitate appropriate positioning of the input beam *vis-a-vis* the scattering. Moreover, the axis of the transducer can also be rotated in the horizontal plane to select the suitable direction of propagation of the input beam. Another part of the angular positioning system is an adjustable arrangement that holds the scatterer as well as positions it centrally as required by the operator. These two things have been taken care of by the 'centering arrangement' as shown in Fig. 2. The third part of the system is the hydrophone and pre-amplifier assembly holder, which is exactly similar to the transducer holder as per as designing is concerned. Nevertheless, the holder is connected to one end of a long arm as shown in Fig. 2. The arm can rotate around the scatterer to receive scattered fields at various angular directions. It has been also made as long as the container can accommodate to receive

scattered fields in the asymptotic region with respect to the characteristic dimension of the scatterer. For our case, the holder is attached with the arm at a distance 170 ± 10 mm from the centre. The pre-amplifier is 60 mm long and therefore if we grip it at the central region by the holder then only < 40 mm space remains as a free space between the wall of the container and back of the pre-amplifier. This space has been left free for electrical cable to reside and smooth operations. Two proper arrangements have also been attached to the system in order to adjust the height and angle (in the horizontal plane) of the receiving hydrophone. One of the most important parts of the system is to connect the shaft of the stepper motor (Sanyo Denki, Japan, Unipolar, step: 1.8°, 0.25A, Type 103G775-1511, Lot number 09609, Serial No. 6037443-2) to another shaft, situated at the other end of the long arm as shown in Fig. 2. These two shafts have been coupled with a belt and backlash free movement can be achieved by adjusting speed of revolution and tension of the belt. This has been accomplished by trial and error method. Moreover, the motor can also move in half step *i.e.* 0.9°, which is indeed required for angular scanning with higher resolution. In addition, two limit switches have been placed on the horizontal bar to avoid collision between the hydrophone and transducer. Finally, screw arrangement has been made in the legs of the system for its proper labeling, which is also a pre-requisite to achieve its mechanical stability.

4 Experimental Results

4.1 Description of ambient medium and various gadgets

The performance of the arrangement has been examined by executing a standard experiment *i.e.* the scattering by a long rigid cylindrical object for which the angular distribution of the scattered amplitude is theoretically known. A block diagram of the whole experimental set-up is shown in Fig. 3. Steel wire of spring grade (Bureau of Indian Standards, specification— 304, 316) has been taken as the prototype cylindrical scatterer. All the experiments have been conducted within a Perspex tank filled with ultra pure water (dissolved oxygen— 9.2ppm at room temperature and conductivity— 0.05 μS cm^{-1}), which happens to be the surrounding medium for the scatterer. The temperature of the room as well as that of water has strictly been maintained at 27°±1°C. An unfocused, circular, resonant transducer (PANAMETRICS-NDT, USA, PART NO.-V325) of diameter 9.6 mm has been used as a source to

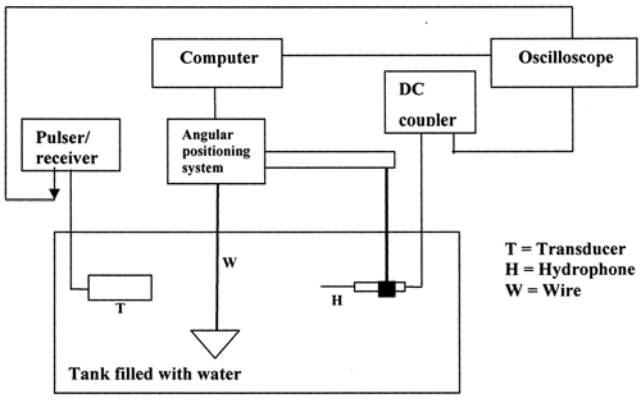

Fig. 3—Block diagrams of various components of the experimental set-up.

irradiate the scatterer. The center frequency of the emitted pulse is ≈ 2.25 MHz with 1.462 MHz (≈ 65%) as the −6dB bandwidth. An ultrasonic square wave pulser/receiver unit (GE Panametrics, Model-5077PR) has been used to drive the transducer at a constant pulse repetition frequency (PRF) of 100 Hz. A piezoelectric polymer polyvinylidene fluoride (PVDF) wideband needle hydrophone (Precision Acoustic Ltd., UK) of diameter 0.5 mm with 9 μm thickness has been employed to receive the scattered signals at various angular directions. The diameter of the hydrophone has been selected as small as possible to minimize spatial averaging over the aperture[10]. Essentially, this choice has been a tradeoff between the aperture effect of the receiving transducer and its sensitivity. The typical hydrophone sensitivity is 300 nV/Pa. The hydrophone has been connected with a submersible pre-amplifier in order to boost the received signals further. The required power for the operation of the pre-amplifier has been supplied by a *dc* coupler, which also filters out the *dc* offset from the received signal. The filtered signal has been taken out from the output terminal of the *dc* coupler and has been fed to the oscilloscope (Tektronics TDS 510B DPO). The oscilloscope has been triggered externally with a square wave of frequency equal to PRF. In addition, the received signals have been sampled by the oscilloscope at the rate of 500 Ms/s. The hydrophone has been placed at different angular positions by using the stepping motor for measurements. The stepping motor of the angular positioning system and the oscilloscope are connected to the computer by RS232 bus and a general-purpose interface bus (GPIB) respectively for synchronized operations. A Matlab code compatible for Version-6.5 has been developed to operate the angular positioning

system as well as to transfer data from the oscilloscope to the computer for recording. The uncorrelated electrical/electronic noise associated with the signals has been removed significantly by averaging the signals over a number (400) of frames[11] where each frame contains signal taken at a time. The required portion of the received signal has been selected by the use of built-in time gating functions (rectangular window) of the oscilloscope. Finally, it is sent to the computer for further analysis. This step has been followed for each measurement. All measurements have been made on a single plane, which contains the axes of the transducer and the hydrophone, situated at a depth 55 mm from the top of the water surface throughout the experiment to avoid any chance of receiving the reflected beam from that surface.

4.2 Reliability assessment of the instrument

The reproducibility and accuracy of the system have been extensively studied[12] before conducting the scattering experiments. In order to perform this study, we have first measured 100 independent signals (each signal averaged over 400 frames) transmitted by the transducer precisely at a particular position with a suitable time gap of 4s and then we have calculated the mean and standard deviation from this set for a number of parameters of our interest. The magnitude of nonzero standard deviation gives a measure of electrical/electronic fluctuations associated with the signals if we assume that the responses of the transmitter and the receiver remain constant or linear throughout the experiment. In the second method, we have again measured the signal at the same position but after one complete to-and-fro excursion around that position. This measurement has been repeated 100 times to calculate the mean and standard deviation for those parameters. Further, between any two successive measurements a time interval of ≈ 60s has been maintained to restore stability within the water medium since it has been disturbed due to the movement of the macroscopic receiving object. The mean values obtained from the above two approaches will certainly differ if the stepping motor acquires backlash errors during its forward and backward motion and also the magnitude of difference reveals the measure of backlash error gathered by the motor. The angular positioning system can be acceptable if the difference between them is negligible i.e. within the order of standard deviation. Table 1 details the statistics based on 100 experimental observations. The first four parameters[13-15], extracted from time gated pulse, of the first column presented in Table 1, namely, the peak to peak amplitude, peak positive (related to the maximum compressional pressure), peak negative (related to the maximum rarefactional

Table 1—Mean and standard deviation of various parameters measured at three different positions

Quantity		Position 1		Position 2		Position 3	
		Electronic fluctuation	Positional fluctuation	Electronic fluctuation	Positional fluctuation	Electronic fluctuation	Positional fluctuation
	Mean (mV)	2.59	2.59	1.37	1.36	67.76	67.61
Peak to peak	Std. deviation (μV)	20	20	20	18	118	136
	Std. deviation in Per cent	0.78	0.79	1.48	1.33	0.17	0.20
	Mean (mV)	1.02	1.02	0.57	0.57	36.00	35.94
Peak positive	Std. deviation (μV)	11.88	14.86	15.54	12.57	88.42	97.22
	Std. deviation in per cent	1.15	1.44	2.69	2.19	0.24	0.27
	Mean (mV)	-1.56	-1.56	-0.79	-0.79	-31.75	-31.67
Peak negative	Std. deviation (μV)	15.03	14.59	12.84	13.72	85.82	92.02
	Std. deviation in per cent	0.95	0.93	1.62	1.73	0.27	0.29
	Mean (mV^2 μs)	0.695	0.691	0.157	0.157	212.411	211.397
Pulse intensity integral	Std. deviation (mV^2 μs)	0.002	0.005	0.001	0.001	0.243	0.573
	Std. deviation in per cent	0.329	0.660	0.834	0.660	0.115	0.271
	Mean (mV)	4.94	4.92	2.14	2.15	70.48	70.28
Amplitude for frequency 2.19 MHz	Std. deviation (mV)	19	22	20	19	102	135
	Std. deviation in per cent	0.39	0.45	0.93	0.90	0.14	0.19

pressure) and pulse intensity integral (related to the energy deposited by a pressure pulse at a space point) are always the quantities of interest in any ultrasonic experiment and specially when one is aiming to use the set-up for biomedical applications. We have also studied the amplitude variations, which is included in fifth row in Table 1, for the incident wave of frequency 2.19 MHz only the angular scattering patterns for that wave are also presented. The information of an incident wave of particular frequency is generally extracted from the short duration pulse emitted by the commercially available medical transducers by employing the Fast Fourier Transform method. The results of three different positions have been presented in Table 1. For first two positions, the signals have been captured by using the oscilloscope at higher gain setting (2 mV/division scale) whereas the same has been done with a lower gain setting (20 mV/division scale) for the third position. If we look at the results for peak-to-peak measurements for position 1 we find that the agreement of the mean values between two methods is excellent and therefore their difference is well within the order of standard deviation. Similar trends more or less are followed for the other parameters too. These are independent of the observation positions and oscilloscope's gain setting. The ratio of standard deviation to mean (expressed in percentage) has also been included in Table 1 for all parameters. Therefore, as reflected from our results, the measured values are reproducible since only <3% variations for all parameters are observed. Further, the stepping motor can quite accurately place the hydrophone at the desired positions and also it does not acquire any observable backlash error during its to-and-fro motion. An experiment has been executed by using a laser beam to cross-check the angular accuracy of the motor and convincing results have been obtained.

4.3 Line scan results

Figure 4 shows the spatial variation of pressure transmitted field amplitude along the radial direction at a distance of 69.04mm from the transducer surface for the emitted wave of frequency 2.19 MHz. This field is indeed the incident field for the scatterer. Both theoretical and experimental results are shown in Fig. 4. The theoretical pattern (represented by line) has been generated by assuming that the source is a plane piston type transducer and hence its far field normalized amplitude is given by, $p(y)=|J_1(ka\sin\varphi)/ka\sin\varphi|$, where $\sin\varphi = y/\sqrt{(x^2+y^2)}$

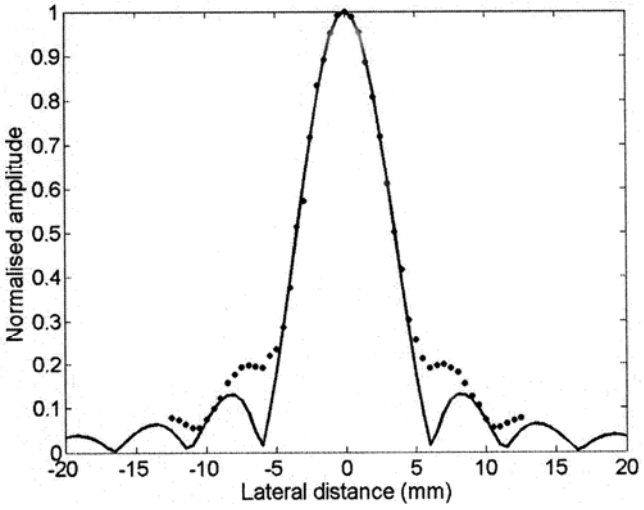

Fig. 4—Normalized field amplitude distribution at a distance 69.04 mm from the center of the transducer along a lateral direction for an unfocused circular transducer of diameter 9.6 mm. Line: Calculated pattern for plane piston type transducer of frequency 2.19 MHz. Points: Corresponding experimentally measured values.

and J_1 is the Bessel function of first order (Ref. 16). Here, the X-axis is taken as the direction of propagation of the incident field.

The spatial variation of the emitted field has been measured by using a 3D positioning system (Mclennan Servo Supplies Ltd., UK) with 25 μm axial resolution. It is note worthy that the beam emitted by the transducer cannot be treated as a plane wave, rather the field amplitude falls off along the lateral direction. This is due to the fact that the size of the active aperture is finite and hence, the amplitude distribution is governed by the diffraction effect. From Fig. 4, it is also clear that the measured values are in good agreement with that of the theoretical values when they belong to the main lobe. The first minimum in both patterns match positionwise although they differ in magnitude. The magnitudes as well as the positions of other maxima and minima also differ in the two patterns. The small discrepancy between the theoretical and experimental patterns can be largely attributed to the fact that the vibration of the real crystal deviates from the plane piston type vibration, which is the underlying assumption of this theoretical model. More precisely, the central portion of the crystal vibrates with greater amplitude than the boundaries.

4.4 Angular scan results

In Fig. 5, the measured angular scattering results for that incident beam of frequency 2.19 MHz are

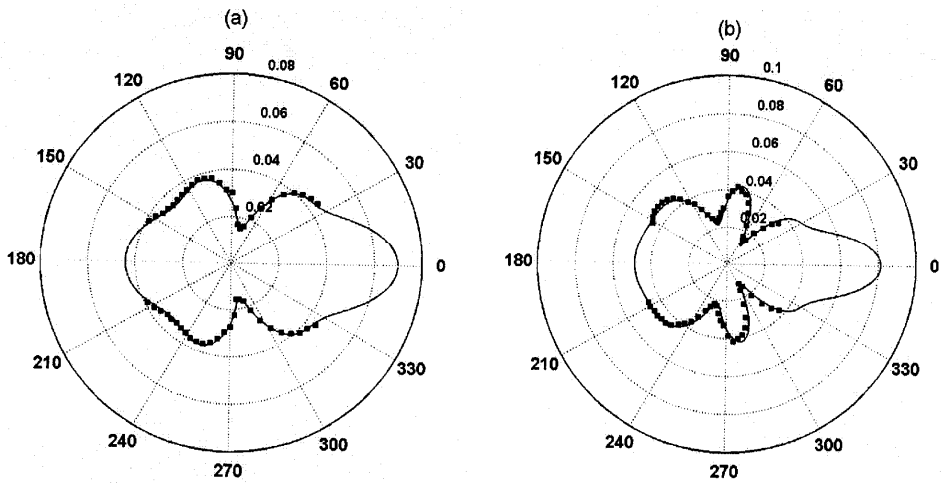

Fig. 5—Normalized (by the amplitude of incident field at the position of the scatterer) angular scattered filed amplitude pattern. (a) Line: Calculated filed amplitude angular distribution when the incident wave is a plane wave of freq 2.19 MHz and the scatterer is steel wire of diameter 0.68 mm with $x \approx 3.12$. Squares: Experimentally measured values when scaled by a factor of 1.7. (b) Same as (a) but for the wire of diameter 0.91mm with $x \approx 4.17$

shown for two cases using wires of different gauges for comparisons with the corresponding theoretical patterns. The normalized angular scattered amplitude has been calculated by using Eq. (2). To carry out the calculation, the quantities such as density, Young's modulus and Poisson's ratio of the scattering object are taken, by consulting standard literature, to be 7850 kg/m^3, 19 GPa and 0.33 respectively. The density and longitudinal sound wave speed through the water medium are also assumed to be 1000 kg/m^3 and 1500 m/s, respectively.

The scattering target has been positioned at the far field (69.04 mm away from the source, where NFZ being ≈ 33 mm), where the spatial variation of the incident field is smooth compared to its near field for the source transducer. In the receiving side, the hydrophone has been stationed at 103.69mm away from the center of the scatterer to ensure that it can receive scattered signals in the asymptotic region with respect to the scattering wires whose diameters are 0.68±0.02 mm and 0.91±0.02 mm, respectively, with size parameters $x \approx 3.12$ and 4.17. Accordingly, the scatterers belong to the Rayleigh region, where the characteristic size of the scatterer is smaller than the wavelength of the interrogating wave. In this context, it may be noted that there are also two regions, namely, stochastic and diffusion regions, where the size of the scatterer is of the order of the wavelength and larger than the wavelength, respectively. The wires have been suspended vertically from the top and positioned properly by using a special centering arrangement as shown in Fig. 2. The receiver can be placed with the help of stepping motor at some discrete positions and in principle on a circle concentric with the scatterer to capture scattered signals.

The measured scattered amplitude has been normalized by the incident amplitude (at the position of the scatterer) in order to match with the theoretical pattern. A factor of 1.7 has been further multiplied with the normalized measured values to bring the experimental results into good agreement with the theory. The reason for this scaling is that the field emitted by a transducer cannot be a plane wave since it has a finite aperture. Therefore, amplitude as well as phase of the incident field varies over the region of the scatterer. However, for plane wave scattering as in the theoretical derivation Eq. (2), the amplitude of the incident wave remains same over the scattering region. As a result of this mismatch between the theoretical model and the real input field, the magnitude of the scattered signal differs from its theoretical value[1]. From Fig. 5(a), it is clear that for the first specimen there is a very good agreement between the theoretical and experimental patterns. However, for the other we observe very small mismatch. This may be due to the misalignment of the normal of the hydrophone's aperture with that of the circular orbit as well as off centering of the scatterer with respect to the centre of rotation of the hydrophone.

Experimental results reaffirm the fact that when the size of the scatterer is much smaller than the central lobe of the interrogating ultrasound beam which is certainly not a plane wave but still the plane wave approximation remains fairly valid. We note, how,

closely the experimental result reproduces the theoretical angular scattering pattern for this input beam.

5 Conclusions

A custom made experimental set-up has been developed for precise measurement of angular and back scattering components from an isolated scatterer or from a bulk sample containing a distribution of scatterers. Both the angular and back scattering techniques are being used widely to study biological tissue materials since these techniques have found tremendous applications in diagnosis and characterization of these samples. Several researchers employed this type of instrument for the measurement of scattering components and by analyzing the scattered signals they quantitatively characterized the scattering medium. For example, similar instruments had been used to investigate *in vitro* scattering by isolated breast tissue lobules[17] and also to study frequency dependent angular scattering from *in vitro* tissue samples to obtain the quantitative information of scatterer properties[18] .

We have examined the efficacy of this set-up extensively with respect to its angular resolution, reproducibility of measured data at a particular spatial coordinate, mechanical stability and immunity to the electrical and acoustical noise. Furthermore, we have measured the angular distribution of the scattered field by a sufficiently long rigid cylindrical scatterer for an incident wave of single frequency. The size of the scatterer is such that it belongs to the Rayleigh scattering region. The information of a particular frequency has been decoded from the scattered pulse by using the fast Fourier transform method since the metallic target has been insonified by a short duration pulse as emitted by a commercially available medical transducer. Two steel wires of different diameters have been used as prototype scatterers. The measured values have been compared with the corresponding theoretical results in order to validate the system. Some of the results of this work have been presented in tabular form and others are displayed through Figures. We can draw the following conclusions based on our investigations.

(i) The stepper motor has worked satisfactorily from the point of view of angular accuracy and most significantly, it does not acquire any observable backlash error during its forward and backward motion; (ii) measured values are reproducible, only very small variations (<3%) have been observed due to electrical/electronic noise; (iii) the system has the flexibility of incorporating transducers of lower and higher frequencies *i.e.* the source holder can move in both directions (near and far) from the centre of the target. This is required to ensure far field scattering; (iv) measurements of scattering components for an isolated particle scattering can be made with the existing set-up; (v) frequency or angle dependent *in vitro* characterization of biological tissue samples containing a poly-disperse distribution of scatterers is also possible with the same instrument; (vi) it can also be employed for the purpose of continuous wave scattering when the walls are padded with acoustic absorbers to avoid multiple scattering from the walls.

Though the instrument at this stage serves our purpose quite efficiently, the authors are aware of the fact that the following scope of improvements exist and can easily be incorporated in the present system:

(i) The transducer holder can be modified to facilitate rotation in the vertical plane along with the corresponding read out facility. This adjustment is some times required for proper alignment of the incident beam; (ii) same modification can be also made to the hydrophone holder for more versatile operations e.g. three-dimensional movements; (iii) a gear arrangement can be introduced to increase the angular resolution, which will be useful for measuring scattered fields with higher spatial variation; (iv) an additional pump arrangement, for pouring water into the tank and taking it out at the end of the experiment, can also be incorporated.

Acknowledgement

Authors would like to thank Mr Jishnu Basu and Mr Robin Dutta of workshop, Saha Institute of Nuclear Physics, for their suggestions during the periods of planning, designing and manufacturing. We also thank Mr Bipin Bihari Dey and Company for manufacturing the whole unit with time-to-time appropriate modifications. Authors are also grateful to Prof. Subodh K Shama and Prof. Binayak Dutta-Roy of Satynedra Nath Bose National Center for Basic Sciences for constant encouragement and helpful discussions throughout the work. One of the authors, Manas K Roy, also likes to thank CSIR for providing financial supports.

References

1 Faran J J, *J Acoust Society of America*, Vol-23(4) (1951) 405.

2 Lynnworth L W, *IEEE Ultrasound, Ferroelectric & Frequency Control*, 22(2) (1975) 71.

3 Etter P C, "*Underwater Acoustics Modelling & Simulation: Principles, Techniques & Applications*", Spon Press, 2003.

4 Dukhin A S & Goetz P J, "*Ultrasound for Characterizing Colloids*", Elsevier Academic Press, 2002.

5 Shung K K, Theme G A, "*Ultrasonic Scattering in Biological Tissue*", CRC Press, 1993.

6 Jones J P, *Acta Electronica*, 26(1-2) (1984) 3.

7 Kadah Y M, Farag A A, Badawi A M & Youssef A-B M, *IEEE Transactions on Medical Imaging*, 15(4) (1996) 466.

8 Njeh C F & Genant H K, *Arthritis Res,* 2(6) (2000) 446.

9 Morse P M & Ingard K U, "*Theoretical Acoustics*", *McGraw-Hill, New York*, 1968.

10 Goldstein A, Gandhi D R & O'Brien William, *IEEE Ultrasound, Ferroelectric & Frequency Control*, Vol-45(4) (1998) 972-979.

11 Li Y, Chen Q & Zagzebski J A, *IEEE Ultrasound, Ferroelectric & Frequency Control*, Vol 51(2) (2004) 146-152.

12 Preston R C, Bacon D R & Smith R A, *IEEE Ultrasound, Ferroelectric & Frequency Control*, Vol 35(2) (1988) 110.

13 Harris G R, *IEEE Ultrasound, Ferroelectric & Frequency Control*, Vol 35(2) (1988) 87.

14 Raum K & William D O'Brien, *IEEE Ultrasound, Ferroelectric & Frequency Control*, Vol 44(4) (1997) 810.

15 Medina L, Moreno E, González G & Leija L, *Revista Mexicana De Física*, 49(6) (2003) 511.

16 Christensen D A, "*Ultrasonic Bioinstrumentation*", (Wiley, New York), 1988.

17 Davros W J, Zagzebski J A & Madsen E L, *J Acoust Society of America*, 80(1) (1986) 229.

18 Burke T M, Blankenberg T A, Siu A K Q, Francis G Blankenberg & Jensen H M, *Ultrasound in Medicine & Biology*, 21(3) (1995) 292.